NEW TRENDS IN THE CRYSTALIZATION of TiO$_2$ NANOTUBE FILMS

Arūnas Jagminas[*], Edita Guzejevaitė-Gaidamauskienė, Algis Selskis, Gediminas Niaura

Center of Physical Sciences and Technology,
A. Gostauto 9, LT-01108, Vilnius, Lithuania.

ABSTRACT

The results of TiO$_2$ nanotube (Ntb) films crystallization in autoclaves of various atmospheres are presented. We found that amorphous TiO$_2$ nanotube arrays crystallized into a pure anatase by autoclaving in ethanol and water vapor. The Ntb films were treated in PTFE-lined vials at 110 - 180ºC temperatures for several hours in the atmosphere of ethanol, water and ethanol-water mixtures. The photocatalytic properties of the vapor-treated films were superior as compared to those produced after the Ntb annealing at 500°C in the atmosphere of ambient oxygen. We show that autoclaving of Ntb results in the formation of hydrous anatase species with a larger **a** and a smaller **c** lattice parameters as determined by Raman and XRD spectroscopes. These findings were confirmed by X-ray diffraction, Raman spectroscopy and photodegradation of methylene blue.

Key words: crystallization, TiO$_2$ nanotubes, Autoclaved treatment, Raman, Photodegradation

INTRODUCTION

Recently, TiO$_2$ nanotube (Ntb) films have become the target of focused investigations on account of their self-ordered structure and unique physico-chemical properties prospective for their applications in water photoelectrolysis, solar cells, Li batteries, sensors, photo catalysis, etc.

Here we present a short overview on the new trends of as-grown titania nanotubes post treatments seeking to improve photoefficiency of charge carriers and extent their absorption edge into the vis-region. In according to Grimes and Mor [1], four generations of TiO$_2$ synthesis by anodizing way can be distinguished. The first work on the growth of highly ordered TiO$_2$ nanotube films in thickness of only less than 0.5 μm has been reported in 2001 [2]. In second generation, the nanotube film thickness has been increased to ~ 7 μm by using the aqueous buffered F-containing solutions [3]. The use of organic Ti anodizing solutions, such as glycerol, formamide, ethylene glycol or dimethyl sulfoxide with fluorides (HF, NH$_4$F, KF, NaF) drastically increased the lengths of

---

[*] e-mail: jagmin@ktl.mii.lt, tf.: +370 52 648891

TiO_2 Ntbs up to 1 mm [4]. Note that in these solutions quite ordered nanotubes array can simply be fabricated throughout the optimization of anodizing process parameters such as the composition of electrolyte, pH, bath temperature, applied voltage value and processing time (*Fig. 1*).

The as-grown TiO_2 Ntbs are usually amorphous and, hence, exhibit negligible photocatalytic activity. To obtain the crystalline phases of anatase or rutile, a high-temperature post-treatment in oxygen ambient is required. However, multiple factors affect the crystallization of TiO_2 species, including size, uniformity, and conditions applied for TiO_2 formation. Noteworthy that in case of long TiO_2 nanotubes, the annealing frequently results in detachment of some parts of film from the substrate. Moreover, the annealing even at 450 – 500 °C, e.g. in a typical temperature region for anatase-TiO_2 Ntb formation, leads to the formation of thin rutile-TiO_2 sub-layer beneath the nanotube film at the Ti surface. This layer hinders the transport of photogenerated electrons to the back contact that severely limits application of crystalline TiO_2 Ntb films.

In recent years various efforts have been made to develop TiO_2 nanocrystals by low-temperature hydrothermal and solvothermal treatment protocols [5,6]. Analogously, it was decided here to use similar treatments for reconstruction and crystallization of amorphous TiO_2 films formed by Ti surface anodizing in NH_4F-containing ethylene glycol solutions. By this way we found that amorphous TiO_2 nanotubes can be successfully converted into the crystalline TiO_2-anatase nanotubes throughout the sonication in a Teflon-line autoclave containing H_2O and EtOH even at 110 °C.
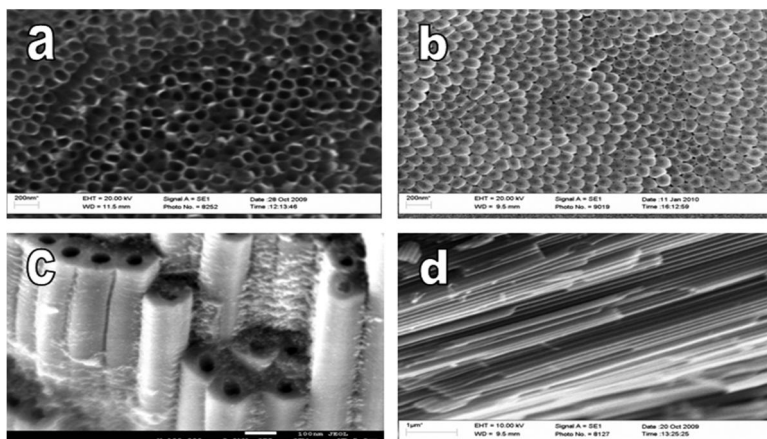

Fig. 1 – Illustrative FESEM images showing topology of a TiO_2 nanotube film fabricated by Ti anodizing in F⁻-containing ethylene glycol electrolyte at 60 V dc and 20 ºC for 3 hr: (a) top-side, (b) back-side, (c) panoramic, and (d) cross-sectional views

We also determined that low-temperature crystallization method allows to escape delamination of TiO_2 Ntb film from the substrate opening new possibilities for their applications.

The composition and morphology of TiO_2 Ntbs after annealing as well as following solvo- and hydro-thermal treatments were studied by XRD, Raman and FESEM.

METHODS

All materials used in this study were purchased from Aldrich as analytical grade reagents and used as received. The 0.125 mm Ti foil (Aldrich, 99.7 at%), was used to prepare 15 ×15 mm^2 specimens. Their surface was ultrasonically cleaned in acetone, ethanol, and water for 3 min in each, and then air dried. The anodization was carried out in a thermostated (20 ±1ºC) glass cell in the 50 ml of electrolyte under stirring conditions. The doubly distilled (DD) water was used throughout. The solution for anodization was ethylene glycol with 20 ml/l of H_2O and 0.3-0.5 wt% of NH_4F. Each sample was anodized in a fresh solution. Two stainless steel plates positioned at 13 mm from the anode were used as cathodes. The 60 V dc voltage was applied for anodizing of all samples. Typically, the anodization time varied from 3 to 20 hours. After anodization, samples were thoroughly rinsed for ~3 min in ethanol and ethanol-water baths and then air-dried. Samples were heat-treated in a PTFE-lined vial placed into the oven (*Zhermack*). The temperature in the oven was raised from 100 to 180 ºC with a 10°C/min ramp. The samples were heated for 5 to 20 h. Various ethanol/water volume ratios ranging from 100:0 to 0:100 were tested. The 25 ml autoclave was filled up with 12.5 ml of the liquid. To avoid direct contact of the sample with the liquid, the sample was placed on a special glass holder. Some experiments were done in D_2O instead of H_2O. For comparison, a few anodized Ti samples were heated in an air oven at 500 ºC for 2 h using a 10 °C/min ramp.

The structure and morphology of TiO_2 nanotube arrays were studied before and after the post-treatments with a field emission scanning electron microscope (FESEM, model Hitachi S-6000). Phase composition of anodized and heat-treated samples were studied by X-ray powder diffraction (XRD) using a D8 diffractometer (Bruker AXS, Germany), equipped with a Göbel mirror as a primary beam monochromator for CuK_α radiation. A step-scan mode was used in the 2Θ range from 18 to 55° with a step-length of 0.02^o and a counting time of 8 s per step. The size of anatase crystallites was determined from the diffraction peak broadening using the Scherrer formula [7].

Raman measurements were performed either with a 632.8 nm excitation (He-Ne laser) by using the Raman microscope LabRam HR800 (Horiba Jobin Yvon) equipped with a grating containing 600 grooves/mm and the CCD detector cooled by the liquid nitrogen, or with a 785 nm excitation using the

Echelle type spectrometer RamanFlex 400 (PerkinElmer, Inc.) equipped with the thermoelectrically cooled (–50 °C) CCD camera and fiber-optic cable. Laser power at the sample was typically 1 mW for the 632.8 nm and 20 mW for the 785 nm excitation. High frequency spectra (1100-3800 cm^{-1}) were recorded with the 5 mW (632.8 nm) laser power. The 632.8 excited Raman spectra were taken using a 50x/0.75 objective lens. Integration time was 50 s. The Raman frequencies were calibrated using a Si sample (520.7 cm^{-1} Raman mode). The Raman frequencies of 785 nm-excited spectra were calibrated by using the polystyrene standard (ASTM E 1840) spectrum. Intensities were calibrated by a NIST intensity standard (SRM 2241). Laser beam was focused to a 200 μm diameter spot on the surface.

The nanotube films prepared by heat and autoclaving treatments were tested for catalytic activity. The photocatalytic activity of the crystalline TiO_2 samples was studied by observation of the degradation of methylene blue (MB) under UV light irradiation at 365 nm for 1.5 hours. The samples of crystallized TiO_2 nanotube films were dispersed in ethanol using sonication for 1 h, and then dried at room temperature for 24 h. The 0.01 g of TiO_2 were again sonicated in 100 ml of aqueous solution of 6.25 μM MB in the dark for one hour to reach the MB adsorption-desorption equilibrium. The resulting suspensions in a quartz photo reactor were exposed to UV irradiation with a UV diode light with the irradiating 26 ± 2 mW light intensity. The 2.5 ml samples were withdrawn from the reactor every 15 min and centrifuged at 8000 rpm for 5 min. The concentration of MB was determined from the UV-vis absorption spectra recorded with a Perkin-Elmer LAMBDA 35 spectrophotometer. The reproducibility of the MB concentration was within 5 %.

RESULTS AND DISCUSSION

In the *figure 2* we show the XRD traces for the TiO_2 nanotube films, which were heated in ethanol, water and their mixture atmospheres at 180 °C for 10 h. In all cases the crystalline anatase formation from the amorphous TiO_2 is also observed.
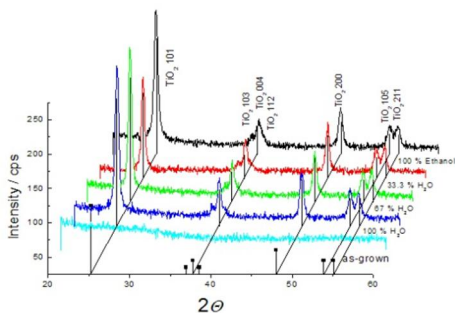

Fig. 2 – XRD patterns of TiO_2 nanotube film before and after autoclaved treatment in the atmospheres of H_2O, EtOH and their indicated mixtures at 180 °C for 10 h. $\partial T/\partial t = 10$ °C/min

Higher crystalline material was formed when the treatment time increased from 5 to 20 h, as suggested by stronger peaks for all main anatase planes in XRD spectra. Surprisingly, the formation of crystalline anatase was observed after the autoclaving of TiO_2 nanotube arrays in various ethanol-water mixture atmospheres even at 110 °C. Higher annealing temperature (T_{ann}) facilitated the formation of higher crystalline product as suggested by increasing diffraction peaks with increasing T_{ann} from 110°C to 180°C. Again, we did not observe any phase changes or impurity peaks appearing in the XRD patterns for the entire temperature range used in our study.

The size of the anatase crystallite for various solvothermal threatment conditions in ethanol are given in *Table 1*. As seen, the crystallite size increased from ~12.9 to 16.5 nm as the processing time increased from 5 to 20 h. Also, we have compared the lattice parameters for autoclaved TiO_2 films with those typical for anatase nanocrystalls (*Table 1*). Our results indicate anatase formation by autoclaving with a lattice parameter a from 0.3795 to 0.3793 nm and parameter c from 0.948 to 0.949 nm. Therefore, in case of autoclaving the lattice parameter a is slightly higher and the lattice parameter c is slightly smaller than those typical for anatase nanocrystalls, the 0.3785 nm (a) and 0.95139 nm (c).

Table 1. Effect of the TiO_2 Ntb film autoclaved treatment conditions in ethanol (~ 96 v/v%) atmosphere on the crystallite size and lattice parameters of anatase

Sample no.	T_{ann}, °C	Crystallite size (d), nm	**a**, Å	**c**, Å	Heat-treatment time, h
1	175	16.48	3.795	9.482	20
2	175	15.54	3.795	9.482	10
3	175	12.94	3.795	9.482	5
4	150	12.45	3.798	9.490	10
5	110	12.92	3.807	9.497	10
Anatase PDF 21-1272	-	-	3.7852	9.5139	

The composition of TiO_2 Ntbs after annealing and sonochemical treatment in H_2O and/or EtOH vapor was further studied by Raman spectroscopy because various titanium oxide phases, including anatase [8], rutile [9], brookite [10], and amorphous state [11] can be discriminated based on specific Raman signatures. It is worth noting that as-grown TiO_2 nanotubes does not show any Raman features characteristic for crystalline TiO_2 phases, instead broad bands near 200, 488, and 614 cm^{-1} indicating the presence of amorphous titanium oxide [11]. We found that amorphous TiO_2 nanotubes can be successfully converted into the crystalline TiO_2-anatase nanotubes throughout the sonication in a Teflon-line autoclave containing H_2O, EtOH or their mixture

even at 110 °C. We also determined that low-temperature crystallization method allows escape the delamination of TiO_2 Ntb film from the substrate.

According to numerous reports, the annealing of amorphous TiO_2 nanotubes film at 450-500 °C results in the crystallization of this material and appearance of strong Raman bands at 144, 397, 517, and 638 cm^{-1} along with the weak feature near 198 cm^{-1} (*Fig. 3a*). All these bands are characteristic of crystalline anatase TiO_2 structure [8]. The dominant band at 144 cm^{-1} we assigned to $E_g(1)$ Raman-active mode, while the peaks at 198, 397, and 638 cm^{-1} belong to $E_g(2)$, $B_{1g}(1)$, and $E_g(3)$ phonon eigenmodes, respectively.

The Raman spectra of TiO_2 nanotube film after hydrothermal and sonochemical treatments considerably differ from the one of calcinated specimen in both the position of the peaks and the width of the bands (*Fig. 3b-d*). In general, Raman bands are considerably broader in the case of autoclaved specimens. Also the $E_g(2)$ mode near 198 cm^{-1}, characteristic for ordering structures, can not be clearly detected. Furthermore, the intense $Eg(1)$ mode was found to be blue shifted by 4.5 cm^{-1} and nearly twice broadened.
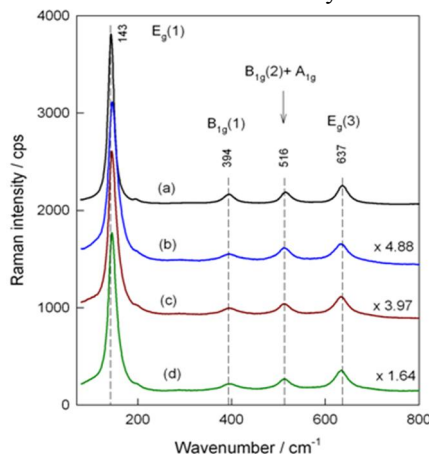

Fig. 3 – Raman spectra of TiO_2 samples in 80-800 cm^{-1} spectral region: heat treated, (b) autoclaved in EtOH, (c) in EtOH:H_2O 1:1 mixture, and (d) H_2O. The excitation wave-length is 633 nm, laser power at the sample 1 mW, and integration time 50 s

We also determined that observed low frequency $E_g(1)$ component in the vicinity of 153-156 cm^{-1} (Fig. 3) can not be explained by reduced crystal size effect, and suggests presence of non-stoichiometry defects due to oxygen deficiency in the autoclaved samples. It was found that intensity ratio of the band near 154 cm^{-1} with respect to one near 145 cm^{-1} ($I_{154}^{Eg(1)}/I_{145}^{Eg(1)}$) increases in the order:

Heat treated (0) < EtOH (0.20) < H_2O (0.21) < EtOH:H_2O (0.27). Thus, Raman data suggest the presence of non-stoichiometry effects for all autoclaved anatases, highest being for EtOH:H_2O sample. In addition, decrease in crystallites dimension below the 10 nm might also take place.

Figure 4 depicts the FESEM and TEM images of TiO_2 nanotubed film produced by Ti anodizing in the ethylene glycol electrolyte containing some higher content of fluoride before (a,b) and after calcinations by heating (c) and autoclaving (d) and the subsequent treatment in ultrasonical bath for 10 min

(e,f). It is worth noting that nanotubes of such films are composed of nanocrystallites in size of several tens of nanometers because the shape, size, and height, as well as the Ntb wall thickness and roughness, all are depended on the composition of solution and anodizing conditions applied. Thus, in the present work we demonstrate that by varying the anodizing and post-treatment conditions the unusual nanotubular/nanocrystalline structure of TiO_2-anatase can be organized.
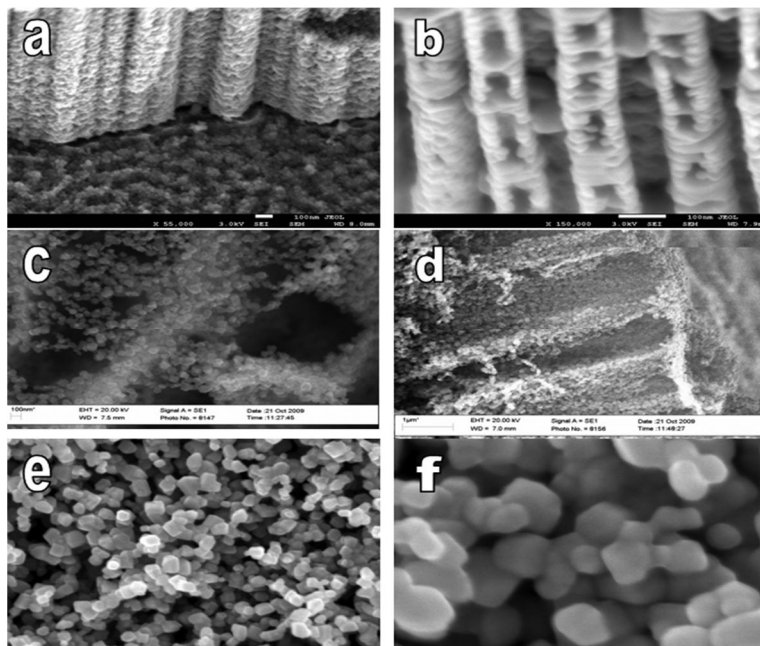

Fig. 4 – Illustrative FESEM (a-d) and TEM (e,f) images showing the topology of as-grown TiO_2 nanotube films in ethylene glycol electrolyte containing 0.4 wt% NH_4F at 60 V and 20 °C for 3 h (a,b) following calcination at 500 °C for 3 h (c,d), and ultrasonication for 10 min (e,f)

Photocatalytic properties of the TiO_2 nanotubed films calcinated by auto-claved and heat-treatments were characterized by the study of decomposition of the methylene blue (MB) dye molecules by TiO_2 species, obtained from calcinated films by ultrasonic agitation. *Figure 5* gives the results. As seen, the MB degradation with TiO_2 calcinated by heat treatment and autoclaving in the isotropic ethanol (~96 %) vapor proceeds rather similar. However, with the increasing time of the ultrasonic agitation, the decomposition efficiency on the TiO_2 samples treated with EtOH was reduced resulting in somewhat lower photocatalytic efficiency compared to the heat-treated samples (see curve 2 in

Figure 5). Surprisingly, significantly faster photocatalytic decomposition of MB dye was observed for autoclaved TiO_2 Ntb film species in H_2O and EtOH–H_2O mixture atmospheres (curves 3 and 4 in *Fig. 5*). A nearly tenfold increase in the degradation rate, as calculated from the slope of the degradation curve was observed for EtOH–H_2O-autoclaved species. *Inset* in *figure 5* compares the kinetic plots of MB photodegradation for various TiO_2 crystallization samples.

It is apparent that photodegradation of MB molecules obeys first-order reaction kinetic as expressed by the equation (1) [12], where t is the reaction time in min and k' is the apparent reaction rate constant in min^{-1}:

$$\ln (C/C_0) = -k't \quad (1)$$

From these plots, anatase species prepared by the autoclaving of TiO_2 Ntb film in EtOH–H_2O (1:1) atmosphere shows the best photodegradation efficiency, reaching the 99.5 % of MB photodegradation after one hour of irradiation, whereas the heat-treated TiO_2 shows only ~65 % of MB photodegradation at similar conditions.
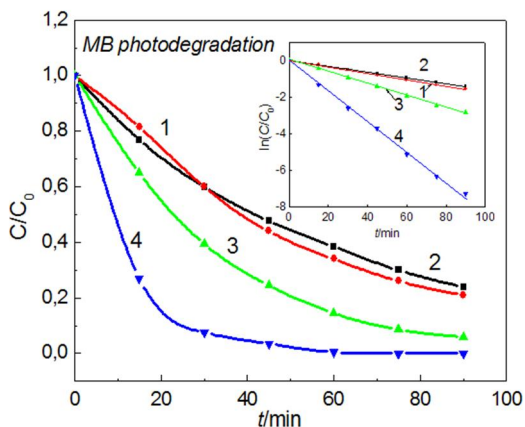
Fig. 5 - Photocatalytic degradation of MB with heat treated (1), and autoclaved TiO_2 species in absolute EtOH (2), pure DD water (3) and EtOH–H_2O (1:1) atmospheres. *Inset:* The semi-logarithmic plots of MB concentration decrease for the same TiO_2 species

CONCLUSIONS

Amorphous TiO_2 Ntb films, produced by Ti anodizing, can be crystallized into pure anatase through a simple and cost-efficient procedure by the film autoclaving in water, ethanol and their mixture atmospheres at 110 to 180°C. The formation of anatase crystals was shown by the X-ray diffraction and Raman spectroscopy. In some cases, the photocatalytic activity of films crystallized in autoclave was advantageous as compared to the TiO_2 Ntb films heat-treated in the air. We expect that the TiO_2 Ntb films prepared by autoclaving in EtOH–H_2O atmosphere can be widely used in future for various photocatalytic applications. The high photocatalytic activity of these films was linked to the formation of the strong Ti–OH bonds with water molecules during the auto-

claving and formation of anatase crystallites with some larger **a** and some lower **c** lattice parameters.

REFERENCES

[1] TiO$_2$ Nanotube Srrays. Synthesis, Properties, Applications (Eds. C.A. Grimes, G.K. Mor). Springer, 2009.

[2] D. Gong, C.A. Grimes, O.K. Varghese et al. J. Mater. Res. 2001, Vol. 16, P. 3331.

[3] J.M. Macak, K. Sirotna, P. Schmuki, Electrochim. Acta, 2005, Vol. 50, P. 3679.

[4] S. Albu, A. Ghicov, J.M. Macak, P. Schmuki, Phys. Stat. Sol. (RRL), 2007, Vol. 1, P. R65-67.

[5] H. Imai, H. Morimoto, A. Tominaga, H. Hirashima, J. Sol-Gel Sci. Tech., 1997, Vol. 22, P. 109.

[6] M. Langlet, A. Kim, M. Audier, J. M. Herrmann, J. Sol-Gel Sci. Tech., 2002, Vol. 25, P. 223-234.

[7] Elements of X-ray Diffraction, (Ed. B.D. Cullity), Addison-Wesley Publishing Company, Inc. London, 1978, P. 99.

[8] M. Mikami, S. Nakamura, Phys. Rev B, 2002, Vol. 66, No 155213.

[9] S.P.S. Porto, P.A. Fleury, T.C. Damen, Phys. Rev., 1967, Vol. 154, P. 522.

[10 G.A. Tompsett, G.A. Bowmaker, R.P. Cooney et al. J. Raman Spectrosc., 1995, Vol. 26, P. 57.

[11] A. Niilisk, M. Moppel, M. Pärs et al. J. Aarik, CEJP, 2006, Vol. 4, P. 105.

[12] T. Zhang, J. Photochem. Photobiol. A:Chem. 2001, Vol. 88, P. 163-167.